

Interface networks in models of competing alliances

T. A. Pereira,^{1,2,*} J. Menezes,^{2,3,†} and L. Losano^{4,‡}

¹*Departamento de Física Teórica e Experimental,
Universidade Federal do Rio Grande do Norte, 59078-970, RN, Brazil*

²*Institute for Biodiversity and Ecosystem Dynamics, University of Amsterdam,
Science Park 904, 1098 XH Amsterdam, The Netherlands*

³*Escola de Ciências e Tecnologia, Universidade Federal do Rio Grande do Norte
Caixa Postal 1524, 59072-970, Natal, RN, Brazil*

⁴*Departamento de Física, Universidade Federal da Paraíba 58051-970 João Pessoa, PB, Brazil
(Dated: February 20, 2017)*

We study a subclass of the May-Leonard stochastic model with an arbitrary even number of species, leading to the arising of two competing partnerships where individuals are indistinguishable. By carrying out a series of accurate numerical stochastic simulations, we show that alliances compete each other forming spatial domains bounded by interfaces of empty sites. We solve numerically the mean field equations associated to the stochastic model in one and two spatial dimensions. We demonstrate that the stationary interface profile presents topological properties which are related to asymptotic spatial distribution of species of enemy alliances far away from the interface core. Finally, we introduce a theoretical approach to model the formation of stable interfaces by means of spontaneous breaking of a discrete symmetry. This allows to write an analytic function for the stationary interface profile. We show that all the results provided by the soliton topological model, presented here for the very first time, are in agreement with the stochastic simulations and may be a powerful tool for understanding the complex biodiversity in Nature. Phase transitions generated by spontaneous symmetry breaking, largely studied in cosmology and condensed matter, may bring light to problems regarding to the coexistence of species.

I. INTRODUCTION

It is well known that the different ways the species interact each other lead to the large variety of biodiversity observed in Nature [1]. Namely, ecosystem dynamics is driven by the spatial patterns arising when different species organize themselves in space [2]. Apart from any climatic conditions, the species form alliances and dispose themselves in space in order to maximize their chances of survival [3, 4].

Early studies in mathematical biology have shown that population dynamics can be understood by means of simple differential equations. In [5, 6], the authors have demonstrated that it is possible to predict the conditions for coexistence of species by searching for the stable states of their populations.

When it comes to space, various numerical stochastic models have been suggested to investigate prey-predator systems [7–24]. Indeed, there is ample evidence that the standard rock-paper-scissors game (three strategies) describes precisely the population dynamics of coral reef invertebrates [25] and lizards in the inner Coast Range of California [26]. Moreover, experimental tests using microbial laboratory cultures of three strains of colicinogenic *Escherichia coli* have shown that even though a cyclic dominance is present, the biodiversity is achieved only when local interactions are considered [27]. As a re-

sult, stable spiral patterns of domains of single species are formed. The same spatial patterns appear in more complex systems with a larger number of strategies [28, 29].

In the case of competing species, numerical stochastic simulations have modeled real biological systems, like interactions among butterflies [30–32]. It has been shown that the dynamics of the interfaces bounding the spatial domains populated by distinct species gives the conditions of coexistence [33–37]. More, it is claimed in [38] that such interfaces, composed by empty spaces, are similar to topological defect networks in cosmology and condensed matter [28, 38–40]. Specifically, the interface network coarsening dynamics is the same as in domain wall networks, where the characteristic scale L grows as $L \propto t^{1/2}$, which characterises a scaling regime [41]. In the case of strings networks in competition models, shown in [42], the network dynamics can be associated with cosmic strings and disclinations in soft matter [43, 44].

In this paper, we focus on the stochastic and topological aspects of interface networks in systems with partnerships. Although some papers have presented some mechanisms of formation of alliances, there is room to investigate partnerships where individuals of different species are indistinguishable. In this case, the interface networks are real generalization of the simplest case with two competing species. We furthermore implement the mean field equations to study the spatial distributions of the populations and compute how the interface network evolves.

Because of the strong similarity with topological defects, we subsequently present a soliton topological model to describe the stationary profile of the interfaces. We

*Electronic address: tiberio@dfte.ufrn.br

†Electronic address: jmenezes@ect.ufrn.br

‡Electronic address: losano@fisica.ufpb.br

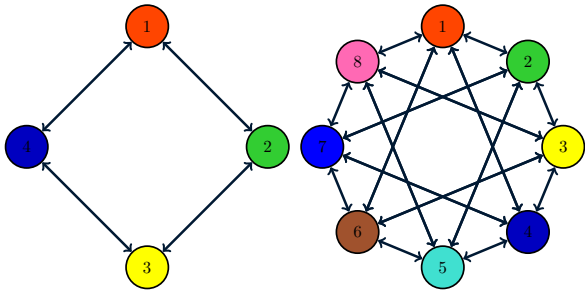


FIG. 1: Illustration of the competition rule for the models with 4 and 8 species are shown in the left and right panels, respectively.

concentrate on spatial patterns formed by means of a phase transition driven by a spontaneous breaking of the discrete symmetry associated to two equally likely alliances. This new formalism may allow the direct comparison of the population dynamics with topological defect networks extensively studied in other scenarios[45–52].

In the next section, we introduce the spatial stochastic model with an arbitrary even number of species that leads to formation of two partnerships of equal individuals. In Sec. III, the mean field equations are introduced and the dynamics of the interface networks is studied. In Sec. IV, the soliton topological model is presented and the stationary profile of the interface is found. In Section V we discuss the results by comparing the theoretical soliton topological model with the numerical implementation of the mean field equations. Finally, our main conclusions are presented in Sec. VI.

II. THE STOCHASTIC MODEL

We consider a class of models with an even number N of species, where individuals of species i compete with individuals of $N/2$ other species. This means that we aim to investigate a sub-family of the general spatial stochastic May-Leonard models ([7]), where species segregate into two alliances of $N/2$ species. Competition interactions are also commonly referred as predation interactions even when species are directly competing each other for natural resources (see for example, [40]).

In our stochastic model, there are three types of interactions: mobility ($i \odot \rightarrow \odot i$), reproduction ($i \otimes \rightarrow ii$) and competition ($i j \rightarrow i \otimes$), with $j = i + k$ where k is an odd number $k < N$. Note that while (\otimes) means an empty site, \odot may be a vacancy or an individual of any species. Competition brings out empty spaces, i.e., whenever one individual dies, the grid point is left empty. Subsequently, this vacancy will be occupied by a new individual created by reproduction of any species.

Figure 1 illustrates the competition rule for $N = 4$ (left panel) and $N = 8$ (right panel). Although each species is labelled by i (or j), the cyclic identification $i = i + lN$,

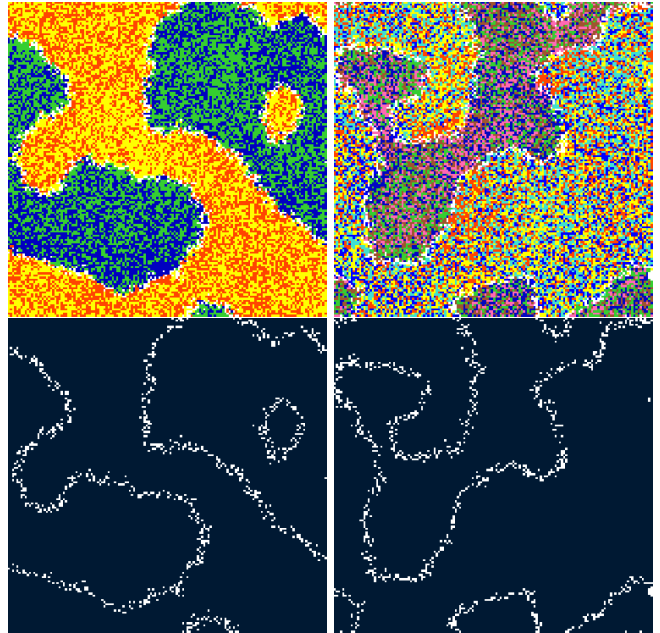


FIG. 2: Snapshots taken from a stochastic numerical simulation of the $N = 4$ (left panels) and $N = 8$ (right panels) models. The upper panels show the spatial domains with partnerships of $N/2$ species, where each individual is colored with the respective color shown in Fig. 1. The white dots represent the empty spaces which form the interface network highlighted in the lower panels.

where l is an integer is assumed. Moreover, all species have the same diffusion, reproduction and competition rates. This implies that, except for the labelling of the different species, schemes in Fig. 1 are invariant under a rotation of $2\pi/N$, leading to a Z_N symmetry.

We performed a large number of stochastic numerical simulations taking two-dimensional networks with \mathcal{N} grid points and periodic boundary conditions. Initially, the number density, $n_i = I_i/\mathcal{N}$ is assumed to be the same for all species while no empty space is present $n_E = I_E/\mathcal{N} = 0$, where I_i and I_E are the total number of individuals of species i and empty spaces, respectively.

At each time step a random individual is sorted to interact with one of its neighbours. After N interactions take place, one generation (our time unit $\Delta t = 1$) is computed. After the initial stage of intense predation activity induced by the random initial conditions, the surviving individuals form two partnerships. The spatial domains populated by individuals of adversary alliances are bounded by interfaces of empty spaces, created by attacks and counter-attacks at the battlefront.

The results presented in this paper were obtained by carrying out simulations with mobility, competition and reproduction probabilities given by $m = 0.25$, $p = 0.50$ and $r = 0.25$, respectively. However, we verified that the same qualitative results remain for other choices of m , p and r .

The upper panels of Fig. 2 show the spatial patterns re-

sulting from the stochastic numeric simulation for $N = 4$ (left panel) and $N = 8$ (right panel), for a 200^2 network. While for $N = 4$ the alliances $\{1, 3\}$ and $\{2, 4\}$ arise, $\{1, 3, 5, 7\}$ and $\{2, 4, 6, 8\}$ are formed for $N = 8$. Individuals of each species are depicted with the same colors shown in Fig. 1. Namely, in the left upper panel of Fig. 2, the alliance of red (species 1) and yellow (species 3) dots compete with the team formed by green (species 2) and blue (species 4) individuals.

In addition, in Fig. 2, white dots represent the empty sites resulting from the competition activities. They form interfaces of vacancies which are highlighted in the lower left and right panels, for $N = 4$ and $N = 8$, respectively. Whenever an individual is killed at the battlefield, the empty space created can be occupied by offspring of any species. However, this new individual can be caught by an enemy which ensures the stability of the interface. Far away from the interface, there is no empty site since individuals belonging to one alliance do not predate each other.

We point out that although the model introduced in [39] also describes the formation of spatial patterns with two competing partnerships, our model presents two crucial differences.

Firstly, while in the model of [39], individuals of various species composing the alliances are homogeneously distributed throughout the respective domains, here the distribution may not be homogeneous. This reflects the way the species interact among them. To be specific, in the stochastic model introduced in [39], each species depends on a specific type of teammate to be protected against death threats. This means that individuals of species i only survive in presence of individuals of species $i - 1$, and they are necessary to the persistence of mates of species $i + 1$. As a consequence, the individuals which have escaped from being chased in the initial stage of the simulation appear surrounded by their saviors, resulting on homogeneous spatial domains. Conversely, in the model presented here all partners provide protection to each other. As a consequence, individuals of species i may be found surrounded by individuals belonging to any species j of the partnership ($j = i + k$, with even k such that $k = 2, 4, 6, \dots, N$). In other words, there is no distinction between the individuals of one alliance. This is the reason why clusters of individuals of the same species can be found in the spatial patterns depicted by the upper panels of Fig. 2.

Secondly, in our model the interfaces do not have internal structures for any number of species N . In contrast, the authors of [39] claim that for $N \geq 8$, stable dynamical structures are formed at the interfaces due to peaceful co-existence of species of enemy alliances. These structures are more complex as N increases. Nonetheless, here individuals of any species compete with everyone from the adversary team. Consequently, there is no room to peaceful arrangements at the interfaces. This leads the formation of interfaces without internal structure for any N , as it is depicted in the right lower panel of Fig. 2 for

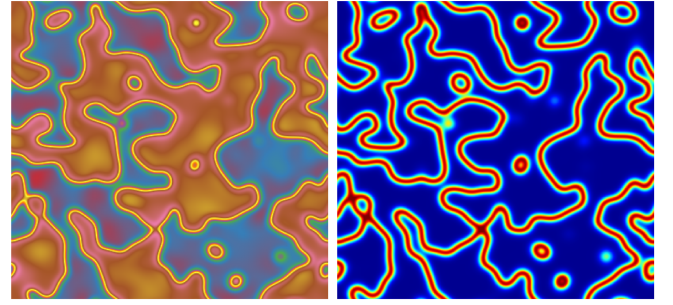


FIG. 3: Snapshots of 400^2 two-dimensional implementation of the mean field equations for $N = 4$. In the left panel, the colors red and blue represent spatial domains occupied by species 1 and 3, while the team of species 2 and 4 occupies the pink and brown regions. The right panel depicts the interface network.

$N = 8$, which allows us to conclude that the model presented in this paper represents a real generalization of interface networks separating two alliances, independent of the number of species.

III. MEAN FIELD EQUATIONS

In this section we aim to describe the spatial population dynamics of our stochastic model by means of a mean field approximation. In this sense, we introduce N real scalar functions $\phi_i(\vec{r}, t)$ (for $i = 1, \dots, N$), which give the portion of space around \vec{r} occupied by species i at time t . In addition, $\phi_0(\vec{r}, t)$ gives the percentage of empty space around \vec{r} at the same instant.

The dynamics of species i is given by

$$\dot{\phi}_i = D \nabla^2 \phi_i + r \phi_0 \phi_i - p \phi_\kappa \sum_j \phi_{i+\kappa}. \quad (1)$$

where $i = 1, \dots, N$ and κ is an odd number so that $\kappa = 1, 3, \dots, N - 1$ and the dot represents a derivative with respect to the physical time. All species have the same diffusion, reproduction and competition parameters, given respectively by D , r and p , where $D = 2m$. The number density of empty space is given by $\phi_0 = 1 - \sum_i \phi_i$.

We solved numerically the mean field equations in two spatial dimensions by taking random initial conditions, where each site is completely occupied by only one species. In other words, we sorted $\phi_i = 1$ for $i = 1, \dots, N$, for each grid point.

The left panel of Fig. 3 shows a snapshot of one 400^2 network, where two spatial domains of $N/2$ species have emerged from the initial well-mixed configuration.

The red and blue regions are dominated by the alliance of odd species $\{1, 3\}$, whereas the team $\{2, 4\}$ populates the pink and brown areas. More precisely, one has $\phi_1 + \phi_3 = 1$ inside the red and blue domains, and $\phi_2 + \phi_4 = 1$ for the pink and brown regions. This yields the non-homogeneous colors seen inside the domains.

The right panel of Fig. 3 shows the interface network of the snapshot in the left panel, where it is highlighted the spatial distribution of number density of empty spaces ϕ_0 . The blue regions are occupied by alliances, such that $\phi_0 = 0$.

It has been shown in [38] that the interfaces tend to straighten in order that their total length decreases in time. As a result, some domains grow while others collapse as a direct consequence of the competition between the partnerships. We notice that either the alliances may coexist in the end of the simulation, or only one invade all territory. In this case, the winner alliance is chosen randomly, since they compete each other with the same parameters. In other words, the surviving species is a result from the random initial network configuration.

A. The interface profile

In order to see how ϕ_0 behaves as the interface, we have solved the mean field equations for one spatial dimension for various values of N . We observe the number density of empty space ϕ_0 at the interface does not depend on the number of species.

For example, for $N = 4$, the one dimensional implementation of the mean field equations started from initial conditions where $\phi_1 + \phi_3 = 1$ for $x < 0$ and $\phi_2 + \phi_4 = 1$ for $x > 0$. After a few number of time steps, competition interactions give rise a stable interface at $x = 0$, as it is shown by the green line of Fig. 4.

This static one-dimensional solution for the number density of empty space is defined as the interface profile. This implies that the interface height H is given by ϕ_0 at $x = 0$. Moreover, at the interface center one has $\phi_1 + \phi_3 = \phi_2 + \phi_4 = (1 - H)/2$. In addition, $\phi_1 + \phi_3 = 1$ and $\phi_2 + \phi_4 = 1$ asymptotically for $x \rightarrow -\infty$ and $x \rightarrow \infty$, respectively. This reveals the topological property of the interface profile, as it is depicted by the blue and red lines of Fig. 4, respectively.

Furthermore, we verified how the interface height depends on the model parameters. To this purpose, we numerically measure H for stable interfaces by varying one of the parameters (D, r, p) while two of them remain constant in their respective values (0.50, 0.25, 0.50). The results shown in Fig. 5 suggest that the larger p the more intense is the predation activity, which leads to a higher interface. Conversely, the more the individuals reproduce (larger r) the lower is the interface. Finally, the inset panel of Fig. 5 shows that if the individuals disperse more (larger D), the interface is also a little bit higher. This happens because they can reach individuals of the enemy alliance easily.

B. The dynamics of the interface networks

We focus now on the macroscopic evolution of the interface networks. Our goal is to find out how the interface

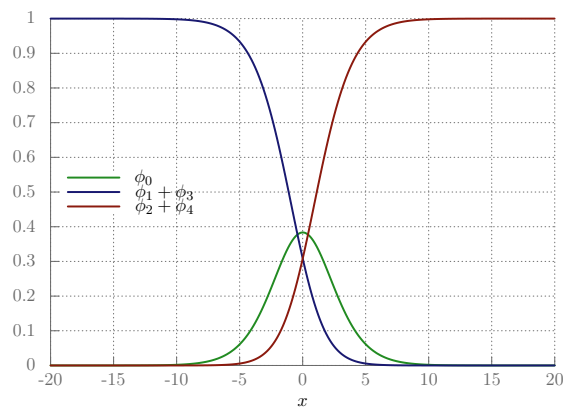


FIG. 4: Stationary solutions for the number density of empty space (green line) and partnerships formed by species $\{1, 3\}$ (blue line) and species $\{2, 4\}$ (red line).

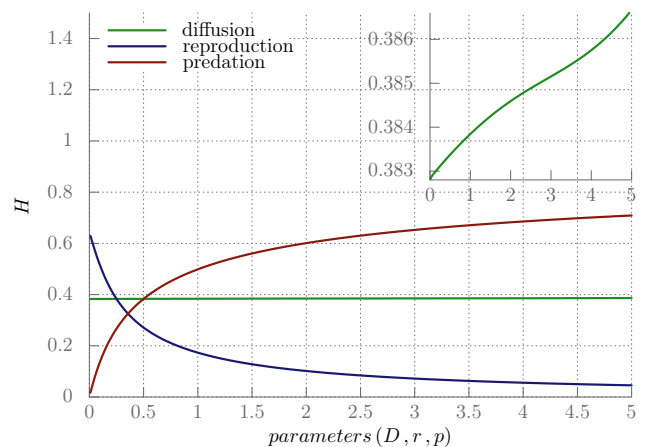


FIG. 5: Variation of the interface height by changing one parameter at a time. The red line shows H for varying p and fixed D and r ($D = 0.50$ and $r = 0.25$). Similarly, the green and blue lines show the results for varying D ($r = 0.25$ and $p = 0.50$) and r ($D = 0.50$ and $p = 0.50$), respectively. The inset panel shows that H changes slightly as D increases.

networks evolve for different values of N .

The characteristic length L of the network is defined as the ratio between the area of the lattice A (the total number of grid points), and the total length of interfaces L_T , i.e., $L = \frac{A}{L_T}$. Given that the interface width is fixed throughout the lattice, the number density of empty spaces per cross section area does not vary. As a consequence, L_T is proportional to the total number of empty spaces. Therefore, L is inversely proportional to the sum of ϕ_0 for the entire network [39].

We computed the average evolution of L with time by running series of 25 two-dimensional mean-field simulations with distinct initial conditions for $2 \leq N \leq 20$. We verified that the scaling law $L \propto t^\lambda$ describes well the late time evolution of the interface networks for any N ,

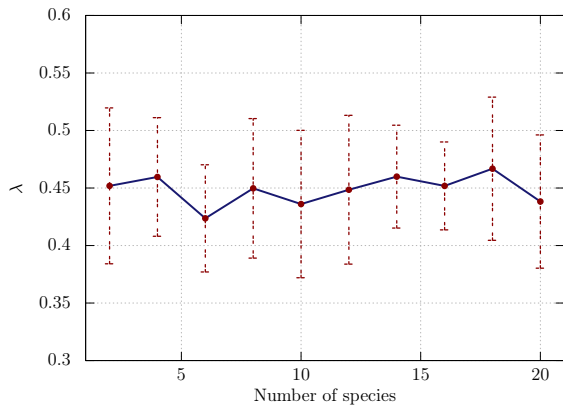


FIG. 6: Scaling exponent for two-dimensional numerical implementations of the mean field for $2 \leq N \leq 20$. The error bars indicate the standard deviation σ^1 of the average value of λ taken from 25 realizations.

which is similar to curvature-driven network evolution of nonlinear systems (see [38]).

The results are shown in Fig. 6 where the error bars indicate the standard deviation σ^1 of the average value of λ . One sees that $\lambda \approx 0.5$, which indicates that the macroscopic evolution of the interface networks is independent of the number of species composing the alliances.

The deviation of λ with respect to 0.5 is also present in previous studies of dynamics of interface networks. For example, in [38] a stochastic version of our simplest case ($N = 2$) is investigated, where the scaling exponent is approximately the same presented here. This shows that our mean field model describes well the dynamics of the stochastic system. However, the reason this significant deviation occurs will be investigated in a further work.

IV. SOLITON TOPOLOGICAL MODEL

In this section we objective to write a soliton topological model to describe the appearance of the interface networks as a result of spontaneous breaking of a discrete symmetry. (see [53]).

The numerical results presented in the previous sections show that an interface is the boundary between spatial regions populated by two adversary alliances. Therefore, we introduce a real scalar field defined as

$$\Phi = \sum_j (\phi_{j+1} - \phi_j) \quad (2)$$

where j is an odd number, such that $j = 1, 3, \dots, N-1$. This allows the replacement of the mean field equations (Eq. 1) by the field equation

$$\dot{\Phi} = D \nabla^2 \Phi - r \phi_0 \Phi. \quad (3)$$

In this approach, the alliances arise for $\Phi(x \rightarrow \pm\infty) = \pm 1$. For example, for $N = 4$ one has $\phi_2 + \phi_4 = 1$ for $\Phi = -1$, while $\Phi = 1$ is assumed when $\phi_1 + \phi_3 = 1$.

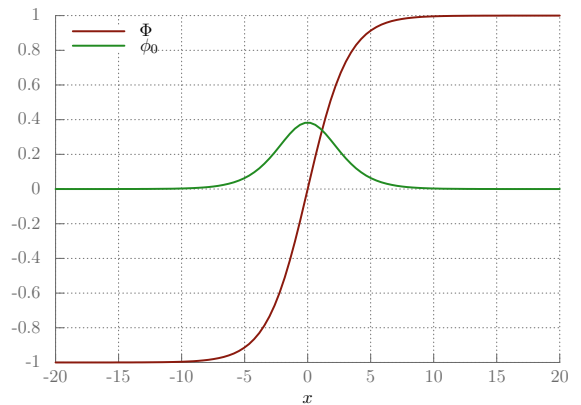


FIG. 7: The red line shows the positive soliton solution $\Phi(x)$ for the static one-dimensional version of the field equation. The stationary interface profile ϕ_0 is represented by the green line.

We highlight that Eq. 3 can be interpreted as the Allen-Cahn equation, which is a reaction-diffusion equation widely used to investigate phase separation in alloy systems (see [54]). In this case, the phase transition is determined by a potential $V(\Phi)$ so that $dV/d\Phi = -r\phi_0\Phi$.

Let us now focus on the one-dimensional static solution of Eq. 3 in order to write an analytic function for the stationary interface profile. Taking into account the existence of two asymptotic partnerships far away from the interface center, we assume the potential with discrete symmetry given by

$$V(\Phi) = \eta (1 - \Phi^2)^2, \quad (4)$$

where η is a function of D , r and p . The interface is the barrier separating the alliances represented by the potential minima $\Phi = -1$ (even species) and $\Phi = 1$ (odd species). Therefore, the static soliton solution for Eq. 3 is

$$\Phi(x) = \pm \tanh \left(\sqrt{\frac{2\eta}{D}} x \right), \quad (5)$$

which asymptotically connect the potential minima. The positive solution represents $(\phi_1 + \dots + \phi_{N-1})$ going from 1 to 0 through the interface, while the negative solution gives the opposite asymptotic behavior. Accordingly, the analytic expression for the interface profile ϕ_0 is

$$\phi_0(x) = H - H \tanh^2 \left(\sqrt{\frac{2\eta}{D}} x \right), \quad (6)$$

whose thickness is given by $\delta \simeq \pi/\sqrt{2\eta}$ (see [55]).

Figure 7 shows the positive solution Φ and the interface profile for the set of parameters assumed in the previous sections. Note that $\eta = Hr/4$, where H is the interface height computed in the one-dimensional implementation of the mean field equations. The parameters η and

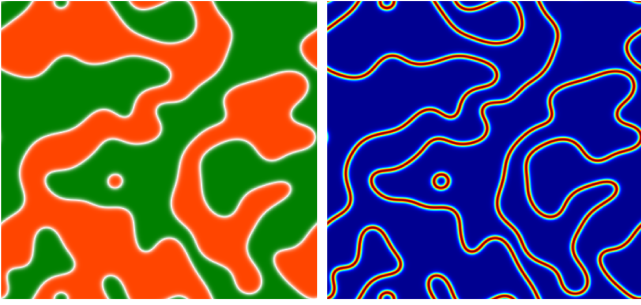


FIG. 8: Snapshots of the implementation of the field equation in a 400^2 two-dimensional network. In the left panel, the colors green and orange represent spatial domains occupied by even and odd species, respectively. The red lines in the right panel show the interfaces.

D determine how fast the solutions reach the potential minima.

We solve numerically Eq. 3 in two spatial dimensions, assuming the potential in Eq. 4. The grid points are given random initial values for the Φ between -1 and 1 .

The well-mixed spatial initial configuration disappears after a few number of step times, when spatial domains of alliances arise. In other words, spatial domains with $\Phi = -1$ or $\Phi = 1$ are created, as it is shown in the left panel of Fig. 8. The domains are bounded by the interfaces shown in the right panel of Fig. 8. The videos in [56] and [57] show how the spatial patterns and the interface network evolves in time, respectively.

Finally, by carrying out 25 numerical implementations of the field equation, we found out that the interface network change in time according to scaling law $L \propto t^\lambda$, with $\lambda = 0.505 \pm 0.16$. This agrees with the results obtained by the numerical implementation of the mean field equations presented in the previous section.

V. CONCLUSION AND DISCUSSION

Performing numerical simulations of a subclass of the more general May-Leonard stochastic model, we found that the spatial patterns show the appearance of spatial regions populated by two competing partnerships. Each member of one partnership is responsible for keeping partners safe and contributing to the territorial advance of the alliance. In other words, there is no distinction between individuals of one partnership. As a result, interface networks without internal structures arise irrespective of the number of species present.

We solve numerically the mean field equations associated to the stochastic model in one and two spatial dimensions. The results described well the spatial patterns provided by the stochastic simulations and the interface profile shows the topological aspects of the system. This means that far away from the interface core, space is occupied for enemy alliances. Based on this, we

presented a theoretical approach where the arising of spatial patterns result from the spontaneous breaking of a discrete symmetry.

The analytic solution of the field equation allows to description of the topological properties of the stationary interface profiles. The spatial patterns resulting from the two-dimensional implementation of this approach strongly agree with the numerical results provided by the mean field model and the stochastic numerical simulations. The dynamics of the interface was also computed by means of the soliton topological model, showing that characteristic length of the interface networks evolve according to the same scaling law of curvature driven system in various nonlinear systems.

We point out that the theoretical soliton model presented here can be also applied to systems with larger number of species, forming N/n partnerships of n species or competing each other ([28, 34]). In this general model the interfaces might join each other in Y-type or N-type junctions. Our model can be used to investigate how the junctions are preferred according to the topological properties of the interfaces ([50]).

Furthermore, this formalism can be generalized to models with competing species whose interactions lead to formation of string networks with and without junctions (see [40, 42]). The same topological issue is present in this case, except for the spatial symmetry engendered by the spatial distribution of the species around the defect cores. In this case, a potential with continuous symmetry is needed, in order that the field equation can describe the formation and evolution of the string networks. The results shown in [42] for the string profile are in complete agreement with the topological structure of the interface profile as a function of the parameters D , r and p .

Our theoretical model may be very helpful to the understanding of population dynamics, since it allows the prediction of the way spatial patterns evolve and how extinction of species and partnerships take place. Combined with the stochastic and mean fields approaches, this formalism may represent an accurate tool to investigate different levels of interaction of individuals and populations in an ecosystem.

Finally we point out that the process of phase transition resulting from a spontaneous symmetry breaking is largely studied in defect networks in Cosmology and Condensed Matter ([43]). The application of the same principles for explaining spatial patterns in Biology constitutes a tool for theoretical researchers, bringing novelty and inspiration to use the physical knowledge to understand old problems regarding to the coexistence among species.

VI. ACKNOWLEDGMENTS

We thank CAPES, CNPQ/Fapern and IBED-Universiteit van Amsterdam for financial support.

-
- [1] R. C. Sole and J. Bascompte, *Self-Organization in Complex Ecosystems* (Princeton UP, Princeton, 2006).
 - [2] M. A. Nowak, *Evolutionary Dynamics: Exploring the Equations of Life* (Harvard University Press, 2006).
 - [3] M. Sabelis, A. Janssen, and J. Takabayashi, *Journal of Plant Interactions* **6**, 71 (2011).
 - [4] G. Szabó and G. Fáth, *Physics Reports* **446**, 97 (2007).
 - [5] A. J. Lotka, *Journal of the American Chemical Society* **42**, 1595 (1920).
 - [6] V. Volterra, *Lecons dur la Theorie Mathematique de la Lutte pour la Vie* (Gauthier-Villars, Paris, (1931)), 1st ed.
 - [7] R. May and W. Leonard, *SIAM Journal on Applied Mathematics* **29**, 243 (1975).
 - [8] B. Kerr, M. A. Riley, M. W. Feldman, and B. J. M. Bohannan, *Nature* **418**, 171 (2002).
 - [9] T. Reichenbach, M. Mobilia, and E. Frey, *Nature* **448**, 1046 (2007).
 - [10] L. Frachebourg, P. L. Krapivsky, and E. Ben-Naim, *Phys. Rev. Lett.* **77**, 2125 (1996).
 - [11] T. Reichenbach, M. Mobilia, and E. Frey, *Phys. Rev. Lett.* **99**, 238105 (2007).
 - [12] J. J. Leisner and J. Haaber, *Proceedings of the Royal Society B: Biological Sciences* **279**, 4513 (2012).
 - [13] H. Cheng, N. Yao, Z. Huang, J. Park, Y. Do, and Y. Lai, *Scientific Reports* **4**, 7486 (2014).
 - [14] A. J. Daly, J. M. Baetens, and B. D. Baets, *Journal of Theoretical Biology* **387**, 189 (2015).
 - [15] A. Dobrinevski, M. Alava, T. Reichenbach, and E. Frey, *Phys. Rev. E* **89**, 012721 (2014).
 - [16] S. Mowlaei, A. Roman, and M. Pleimling, *Journal of Physics A Mathematical General* **47**, 165001 (2014).
 - [17] S. Mowlaei, A. Roman, and M. Pleimling, *Journal of Physics A: Mathematical and Theoretical* **47**, 165001 (2014).
 - [18] A. Szolnoki and M. Perc, *New Journal of Physics* **17**, 113033 (2015).
 - [19] M. F. Weber, G. Poxleitner, E. Hebisch, E. Frey, and M. Opitz, *Journal of The Royal Society Interface* **11**, 20140172 (2014).
 - [20] D. Grošelj, F. Jenko, and E. Frey, *Phys. Rev. E* **91**, 033009 (2015).
 - [21] B. Intoy and M. Pleimling, *Phys. Rev. E* **91**, 052135 (2015).
 - [22] G. Szabó, K. S. Bodó, B. Allen, and M. A. Nowak, *Phys. Rev. E* **92**, 022820 (2015).
 - [23] A. Roman, D. Dasgupta, and M. Pleimling, *Journal of Theoretical Biology* **403**, 10 (2016).
 - [24] L.-L. Jiang, T. Zhou, M. Perc, and B.-H. Wang, *Phys. Rev. E* **84**, 021912 (2011).
 - [25] J. B. C. Jackson and L. Buss, *Proc. Natl Acad. Sci. USA* **72**, 5160 (1975).
 - [26] B. Sinervo and C. M. Lively, *Nature* **380**, 240 (1996).
 - [27] B. C. Kirkup and M. A. Riley, *Nature* **428**, 412 (2004).
 - [28] P. P. Avelino, D. Bazeia, L. Losano, J. Menezes, and B. F. Oliveira, *Phys. Rev. E* **86**, 036112 (2012).
 - [29] M. Boerlijst and P. Hogeweg, *Physica D: Nonlinear Phenomena* **48**, 17 (1991).
 - [30] G. Lei and I. Hanski, *Journal of Animal Ecology* **67**, pp. 422 (1998).
 - [31] M. Zalucki and R. Kitching, *Oecologia* **53**, 201 (1982).
 - [32] J. C. W. K. Elias M, Gompert Z, *PLoS Biol* **6**, e300 (2008).
 - [33] A. Roman, D. Konrad, and M. Pleimling, *Journal of Statistical Mechanics: Theory and Experiment* p. P07014 (2012).
 - [34] A. Roman, D. Dasgupta, and M. Pleimling, *Phys. Rev. E* **87**, 032148 (2013).
 - [35] G. Szabó, *Journal of Physics A: Mathematical and General* **38**, 6689 (2005).
 - [36] G. Szabó and T. Czárán, *Phys. Rev. E* **64**, 042902 (2001).
 - [37] A. F. Lütz, S. Risau-Gusman, and J. J. Arenzon, *Journal of Theoretical Biology* **317**, 286 (2013).
 - [38] P. P. Avelino, D. Bazeia, L. Losano, and J. Menezes, *Phys. Rev. E* **86**, 031119 (2012).
 - [39] P. P. Avelino, D. Bazeia, L. Losano, J. Menezes, and B. F. de Oliveira, *Phys. Rev. E* **89**, 042710 (2014).
 - [40] P. P. Avelino, D. Bazeia, J. Menezes, and B. de Oliveira, *Physics Letters A* **378**, 393 (2014).
 - [41] J. J. Arenzon, A. J. Bray, L. F. Cugliandolo, and A. Sicilia, *Phys. Rev. Lett.* **98**, 145701 (2007).
 - [42] P. Avelino, D. Bazeia, L. Losano, J. Menezes, and B. de Oliveira, *Physics Letters A* **381**, 1014 (2017).
 - [43] E. P. S. S. A. Vilenkin, *Cosmic Strings and Other Topological Defects* (Cambridge University Press, 1997).
 - [44] B. F. de Oliveira, P. P. Avelino, F. Moraes, and J. C. R. E. Oliveira, *Phys. Rev. E* **82**, 041707 (2010).
 - [45] J. Stavans and J. A. Glazier, *Phys. Rev. Lett.* **62**, 1318 (1989).
 - [46] J. A. Glazier and D. Weaire, *J. Phys. Cond. Mat.* **4**, 1867 (1992).
 - [47] H. Flyvbjerg, *Phys. Rev. E* **47**, 4037 (1993).
 - [48] C. Monnerau and M. Vignes-Adler, *Phys. Rev. Lett.* **80**, 5228 (1998).
 - [49] D. Weaire and R. Hutzler, *The physics of foams* (Oxford University Press, Oxford, 2000).
 - [50] P. P. Avelino, C. J. A. P. Martins, J. Menezes, R. Menezes, and J. C. R. E. Oliveira, *Phys. Rev. D* **78**, 103508 (2008).
 - [51] P. P. Avelino, R. Menezes, and J. C. R. E. Oliveira, *Phys. Rev. E* **83**, 011602 (2011).
 - [52] G. W. Semenov, V. Semenov, and F. Zhou, *Phys. Rev. Lett.* **101**, 087204 (2008).
 - [53] R. Rajaraman, *Solitons and Instantons: An Introduction to Solitons and Instantons in Quantum Field Theory*, North-Holland personal library (1982).
 - [54] S. Bartels, *Numerical Methods for Nonlinear Partial Differential Equations* (Springer International Publishing, 2015).
 - [55] W. H. Press, B. S. Ryden, and D. N. Spergel, *Astrophys. J.* **347**, 590 (1989).
 - [56] URL <https://youtu.be/81kbuXUgXeg>.
 - [57] URL <https://youtu.be/RW-ZeeS2QHc>.